Academic Journal of Emerging Technologies
ISSN Print: 3104-4417
ISSN Online: 3104-4425
CD ISSN: 3104-4433
https://doi.org/10.63313/AJET.9017

Experimental Study on Laser Pulse Delay Machining of IN718 Assisted by Chemical Liquid

Fan Liu[1.2.3]. Shufeng Sun[1.2.3.*] and Junbao Li[1.2.3]
[1]Discipline lnnovation and Wisdom Introduction Base of High-end Laser Intelligent Manufacturing Technology and Equipment, Qingdao University of Technology, Qingdao 266525, China
[2]Shandong Provincial Key Laboratory of Laser Green Intelligent Manufacturing Technology, Qingdao University of Technology, Qingdao 266525, China
[3]Qingdao University of Technology, Qingdao 266525, China
Email: sunshufeng@qut.edu.cn

How to cite this paper: Liu, F., Sun, S. F., & Li, J. B. (2025). Experimental Study on Laser Pulse Delay Machining of IN718 Assisted by Chemical Liquid. Academic Journal of Emerging Technologies, 1(3), 9-17. ISSN Print: 3104-4417; ISSN Online: 3104-4425.
https://doi.org/10.63313/AJET.9017
Published: 2025-11-05

Abstract

IN718, a typical nickel-based superalloy, is widely used in critical components such as aero-engine turbine blades and combustion chambers due to its excel-lent high-temperature strength, creep resistance, and corrosion resistance. However, the material's high-temperature strength deficiency, low thermal conductivity, and poor plasticity lead to low efficiency in conventional ma-chining processes and severe tool wear. Laser machining, with its advantages of high energy density, non-contact processing, and flexibility, is regarded as an effective method for machining micro-holes in superalloys. Nevertheless, laser micro-hole machining in ambient air still faces challenges such as oversized hole diameters, rough hole walls, wide heat-affected zones, and thick oxide layers. To address these issues, this study proposes the use of a chemical-assisted machin-ing environment combined with a pulse delay technique, aiming to thoroughly investigate its mechanism and effectiveness in the micro-hole machining of IN718 alloy.

Keywords

Back-jet Processing; pulse-delay modulation; Chemical-Assisted Laser Machining; Microhole Morphology

1. Introduction

With technological advancements, the demand for microholes is continuously growing [1]. Microholes are widely used in fields such as aerospace [2,3], biomedicine [4-6], electronics [7,8], and automotive [9,10]—for example, in turbine blade film cooling holes [11], inkjet printer nozzles [12], bone tissue scaffolds, printed circuit board micro-vias , and fuel injectors ,Currently, the primary methods for microhole machining include electrical discharge machining (EDM) , electrochemical machining (ECM) , and laser machining . EDM is a non-contact machining technique that offers good processability for difficult-to-machine conductive materials, regardless of their hardness or toughness . Moreover, it generates a thinner recast layer compared to other methods. However, it should be noted that EDM inevitably leads to electrode wear and debris formation , and the machining speed decreases as the depth increases . Under the influence of debris, short circuits and secondary discharges occur frequently, resulting in uncontrollable geometric accuracy [.ECM can produce microholes free from microcracks, recast layers, and heat-affected zones , achieving depth-to-diameter ratios of up to 100 . However, during electrochemical drilling, defects such as pitting and "double-eyelid" holes can occur at the hole entrance and along the wall . Additionally, machining efficiency decreases, different workpiece materials require different electrolytes, and electrode fabrication demands high precision . Defects such as spatter and hole blockage may also arise .On the other hand, compared to long-pulse laser drilling, short-pulse laser microhole machining helps reduce the recast layer . The material removal mechanism in short-pulse laser processing involves both photothermal and photochemical effects . Short-pulse lasers offer superior machining quality and accuracy compared to long-pulse lasers . Researchers can optimize scanning strategies to minimize heat accumulation ; however, due to the inherent limitations of short-pulse lasers, defects such as heat effects, recast layer formation, and microcracks cannot be entirely eliminated.Ultra-short pulse lasers, with pulse widths below 12 ps [1], such as femtosecond laser drilling, enable material removal in the form of plasma through rapid expansion of high-density ion-electron gas that overcomes the material’ s binding forces . This improves machining defects such as the heat-affected zone, recast layer, and cracks . However, the material removal rate is relatively low, approximately 0.054 mm^3 /min . To address issues in laser microhole machining such as hole taper , roundness efficiency , hole wall quality heat-affected zone , microcracks , and spatter , researchers have conducted optimization studies focusing on laser parameters, machining strategies, and physical field-assisted methods. Among these, physical field-assisted laser drilling refers to a processing method where the laser interacts with at least one other physical field during the drilling process. This approach can enhance both the quality and efficiency of laser drilling, creating a synergistic effect where 1+1>2. Therefore, it is necessary to adopt physical field-assisted techniques to eliminate the aforementioned defects in laser machining, improve processing efficiency, and achieve high-quality microholes.

2. Experimental details

2.1. Design of a Laser Pulse Delay Machining Scheme with Liquid Assistance

Under the extreme high-temperature conditions generated by the laser, the substrate undergoes an oxidation reaction with oxygen, producing oxides such as NiO, Ni_2O_3, Cr_2O_3, and Fe_3O_4 that adhere to the material surface. These oxides typically deposit at the hole wall or entrance, leading to increased wall roughness or irregular hole geometry, thereby compromising the microhole’ s dimensional accuracy. The presence of the oxide layer also introduces crack initiation sites, reducing the material's fatigue resistance and impact toughness. Under high-temperature or high-stress conditions, the oxide layer may spall, resulting in structural failure of the microhole. Furthermore, for subsequent processes such as electroplating, welding, or coating, the oxide layer can cause reduced adhesion or poor interfacial bonding.Acidic solutions can effectively promote the dissolution of metal oxide layers. Halogen elements, such as chloride ions, exhibit strong complexing ability, exposing the oxide layer directly to the acidic environment and forming soluble complexes with metal ions, thereby disrupting the oxide layer’s integrity and accelerating its removal. In this study, hydrochloric acid (HCl) solution is selected as the reactive medium. The hydrogen ions (H^+) provide the acidic environment, while chloride ions (Cl^-) weaken the stability of the metal oxide layer through complexation, facilitating its dissolution into soluble metal salts. However, although HCl alone can remove certain oxides, its effectiveness against stable oxides such as Cr_2O_3 and CoO is limited. Moreover, it may cause localized corrosion of the substrate, which is detrimental to uniform removal.To enhance both the dissolution efficiency and uniformity of oxide removal, nitrate ions (NO_3^-) are introduced as an oxidizing agent to augment the action of HCl. In an acidic (H^+) environment, NO_3^-dissociated from sodium nitrate acts as a strong oxidizer. Through a synergistic oxidation-complexation mechanism, it significantly improves the dissolution of stubborn oxide layers. For instance, under strong acidic conditions, NO_3^- effectively oxidizes Cr(III) to Cr(VI), promoting the dissolution of otherwise resistant oxides. To mitigate severe corrosion caused by high concentrations of H^+, sodium nitrate ($NaNO_3$)—a neutral salt—is mixed with HCl to form the corrosive solution. This mixed solution exhibits negligible corrosion on the substrate at room temperature but effectively accelerates oxide removal upon heating, while avoiding the localized pitting associated with HCl alone.A back-jet chemical assistance configuration is adopted, combined with the optimal parameters from Chapter 4 for water-assisted processing: laser power 200 W, repetition frequency 20 kHz, scanning speed 100 mm/s, number of passes 60, hatch spacing 20 μm, defocus amount -1 mm, and water layer position at 0.5 mm. The upper surface of the workpiece is exposed to air, while the lower surface and sidewalls are in contact with the liquid, forming a "back-side" chemical environment. The nozzle is positioned approximately 10 mm below the workpiece, ejecting the chemical solution upward toward the back of the workpiece at a flow rate of 30 L/h, maintaining a continuous circulating flow.

3. Optimization of Chemical-Assisted Laser Machining Parameters Using Response Surface Methodology

During the experimental design process, a key challenge lies in determining the functional relationship between the target parameter *y* and the set of factor variables x_1, x_2, … x_n. However, the numerous factor variables introduce uncertainty in their effects on the parameter, and each variable may interact with others, leading to potential cross-coupling relationships. Experimental design involves using available tools or methods to plan and conduct experiments, followed by organizing and analyzing the collected data. This enables the acquisition of desired variable values and identifies pathways for improvement and optimization [75].Response Surface Methodology (RSM), proposed by Box et al. [102], is a scientific experimental approach that employs nonlinear fitting and response surface plotting to derive the optimal response value and its corresponding variable settings. Compared with the Central Composite Design (CCD), the Box-Behnken Design (BBD) selected in this study requires fewer experimental runs and offers a simpler combinatorial design.Based on the results of single-factor experiments, the microhole morphology quality score was taken as the response variable. Four factors with significant influence on the quality score—laser average power, pulse delay time, repetition frequency, and scanning speed—were selected as independent variables. Using Design-Expert 11 software, a four-factor, three-level experimental design was implemented. The factors and their corresponding levels are presented in Table 1.

Table 1. Surface response experimental factors and levels

Factor	Factor Levels		
	Low level（-1）	Center Point （0）	High level（1）
Laser power A/（W）	160	180	200
Delay time B/（ms）	75	100	125
FrequencyC/（kHz）	25	50	75
Scanning speedD/（mm/s）	75	100	125

The experimental runs were designed using Design-Expert software. All experiments in this study were conducted in triplicate, resulting in a total of 29 sets. A confocal microscope was employed to characterize the microhole morphology and collect various measurement data. Each set of experiments was measured three times, and the average value was taken as the final microhole morphology quality score. The experimental data and variables were fitted using a polynomial approach. The relationship between the response value Y and the number of variables k can be expressed by the following first-order and second-order equations:

$$Y = \beta 0 + \sum_{i=1}^{k} \beta i \, xi$$

$$Y = \beta 0 + \sum_{i=1}^{k} \beta i xi + \sum_{i=1}^{k} \beta ii xi + \sum_{\substack{i=1 \\ i}}^{k} \beta ij xi \, xj$$

In the given equation, β_0, β_i, and β_{ii} represent the offset term, linear offset coefficient, and second-order offset coefficient, respectively, while β_{ij} denotes the interaction coefficient. Based on the experimental results presented in Table 2, Design-Expert 11 software was employed to develop the model and perform significance analysis. An analysis of variance (ANOVA) was conducted on the test results of the microhole morphology quality score, yielding the following quadratic polynomial regression equation:

$$Y = 84.84 - 0.5A + 2.85B - 0.3917C + 0.3083D - 0.5AB - 0.075AC - 0.025AD - 0.175BC - 0.125BD - 0.125CD - 5.16A^2 - 5.33B^2 - 2.95C^2 - 0.07D^2$$

Table 2. Experimental scheme and results

Experimental Run	Laser powerA/（W）	Delay timeB/（ms）	Frequency C/（kHz）	Scanning speedD/（mm/s）	Mass Fraction
1	160	75	50	100	70.4
2	200	75	50	100	70.6
3	160	125	50	100	77.2
4	200	125	50	100	75.4
5	180	100	25	75	80.7
6	180	100	75	75	80.1
7	180	100	25	125	81.9
8	180	100	75	125	80.8
9	160	100	50	75	79.0
10	200	100	50	75	77.8
11	160	100	50	125	79.4
12	200	100	50	125	78.1
13	180	75	25	100	73.1
14	180	125	25	100	78.9
15	180	75	75	100	72.5
16	180	125	75	100	77.6
17	160	100	25	100	76.4
18	200	100	25	100	75.6
19	160	100	75	100	76.0
20	200	100	75	100	74.9
21	180	75	50	75	75.1
22	180	125	50	75	81.2
23	180	75	50	125	75.9
24	180	125	50	125	81.5
25	180	100	50	100	83.8
26	180	100	50	100	83.7
27	180	100	50	100	83.9
28	180	100	50	100	84.0
29	180	100	50	100	83.8

The P-value (Probability) represents the probability that noise could produce an erroneous result. The magnitude of the P-value indicates the significance of the correlation coefficient in the test. As shown in the ANOVA results of the regression model in Table3, the model's P-value is less than 0.0001, demonstrating that the model is highly significant and valid. The lack-of-fit term is not significant ($P = 0.1012 > 0.05$), indicating that the functional relationship between the investigated factors and the response value is highly significant, with almost no lack-of-fit phenomenon, and the equation exhibits a good fit.The coefficient of determination R^2 and the adjusted R^2 adj are 0.9987 and 0.9975, respectively, suggesting that the model has a high goodness-of-fit and small experimental errors, making it suitable for the optimization and prediction of microhole morphology quality. The high correlation between actual and predicted values further supports this. Therefore, the model effectively reflects the relationship between various factors and the response value in the preparation of high-quality microholes and can reliably predict the optimal process conditions. Based on the P-values, all linear terms (A, B, C, D), the interaction term AB, and the quadratic terms (A^2, B^2, C^2) have a highly significant impact on the microhole morphology quality score ($P < 0.01$), while the remaining terms are not significant ($P > 0.05$). According to the F-values, the order of influence of the four factors on the microhole morphology quality score is: B > A > C > D, i.e., pulse delay time > laser power > repetition frequency > scanning speed.

Table 3. Quadratic polynomial model ANOVA for micro-holes mass fraction

Source	Sum of Squares	Mean Square	F-value	p-value
Model	438.33	31.31	785.78	< 0.0001
A	3.00	3.00	75.29	< 0.0001
B	97.47	97.47	2446.21	< 0.0001
C	1.84	1.84	46.20	< 0.0001
D	1.14	1.14	28.63	0.0001
AB	1.0000	1.0000	25.10	0.0002
AC	0.0225	0.0225	0.5647	0.4648
AD	0.0025	0.0025	0.0627	0.8059
BC	0.1225	0.1225	3.07	0.1014
BD	0.0625	0.0625	1.57	0.2309
CD	0.0625	0.0625	1.57	0.2309
A2	172.54	172.54	4330.24	< 0.0001
B2	184.45	184.45	4629.08	< 0.0001
C2	56.26	56.26	1411.90	< 0.0001
D2	0.0318	0.0318	0.7977	0.3869
Residual	0.5578	0.0398		
Lack of Fit	0.5058	0.0506	3.89	0.1012
Pure Error	0.0520	0.0130		
Cor Total	438.89			
R2	0.9987			
R2Adj	0.9975			

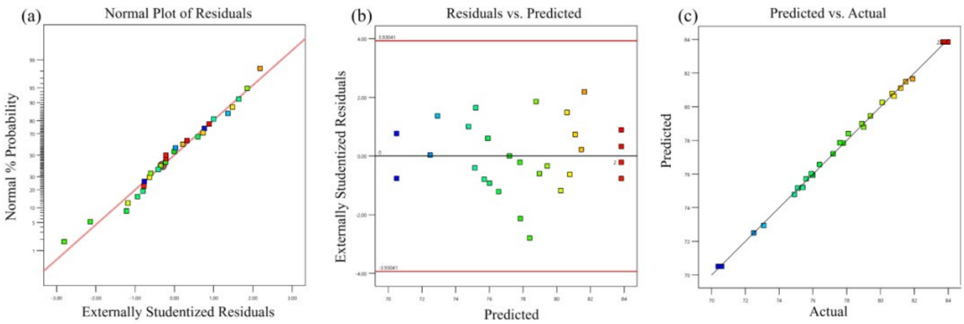

Fig 1. (a) Residual normality plot; (b) Residuals vs. predicted values; (c) Actual vs. predicted values

Figure 1 displays the model adequacy check diagrams generated by Design-Expert software. As observed in Figure 1(a), the residuals are predominantly distributed along a straight line. Figure 5.6(b) shows a random distribution of residuals versus predicted values, while Figure 1(c) demonstrates strong agreement between actual and predicted values. These results indicate that the response surface methodology model, which correlates laser process parameters with microhole morphology quality, is well-suited for this experimental study.

Using Design-Expert 11 software for experimental data optimization and prediction, the microhole morphology quality score was predicted to be 84.0428 under the following process parameters: laser power of 179.198 W, pulse delay time of 111.549 ms, repetition frequency of 47.1687 kHz, and scanning speed of 85.2495 mm/s.In practical operation, adjusted parameters were applied with a laser power of 179 W, pulse delay time of 112 ms, repetition frequency of 47 kHz, and scanning speed of 85 mm/s. The measured microhole morphology quality score was 83.8 $\pm$ 0.2, which is in close agreement with the predicted value. This result demonstrates the model's effectiveness and reliability for process optimization of microhole morphology quality.

4. Conclusion

The back-jet high-temperature chemical-assisted laser pulse delay machining technology provides a one-step solution for eliminating defect layers and optimizing hole geometry, thereby addressing the key challenges of poor surface roughness and extensive hole shape defects. The final morphology is shown in Figure 5.13. This method employs an environmentally friendly chemical liquid that chemically etches the interface of the material's modified layer in a localized high-temperature environment, effectively minimizing surface roughness while removing the oxide and recast layers. Furthermore, the chemical liquid also functions as a confinement layer, restricting the expansion of high-temperature gases and plasma. This confinement leads to an increase in laser plasma ablation pressure, simultaneously leveraging the benefits of liquid assistance and pulse delay characteristics while allowing the chemical reactions to fully realize theiradvantages.

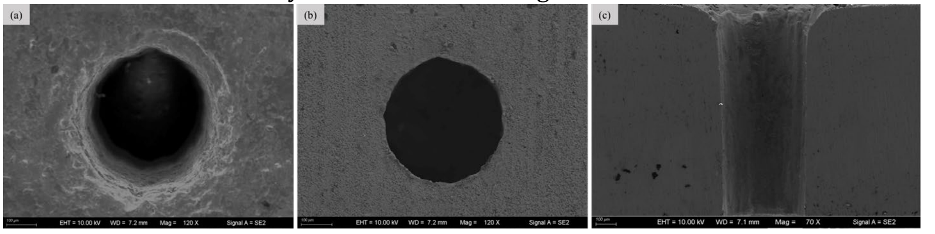

Fig 2. Morphology of back-jet chemical-liquid-assisted laser pulse-delayed drilled micro-hole: (a) Inlet morphology; (b) Outlet morphology; (c) Hole wall morphology

Acknowledgements

This work was support by 111 project of China [D21017]; Shandong Provincial Key Research and Development Program (International Science and Technology Cooperation) [No.2024KJHZ002]; Natural Science Foundation of Shandong Province [No. ZR2023ME156]; "Double Hundred Plan" Talent Program of Shandong Province [WSR2023055]; National Natural Science Foundation of China [52405492]; Qingdao Natural Science Foundation [25- 1-1-207-zyyd-jch].

References

[1] Zhao W, Yu Z. Self-cleaning effect in high quality percussion ablating of cooling hole by picosecond ultra-short pulse laser[J]. Optics and Lasers in Engineering, 2018, 105: 125-131.

[2] Liu C, Zhang X, Gao L, et al. Feasibility of micro-hole machining in fiber laser trepan drilling of 2.5D Cf/SiC composite: Experimental investigation and optimization[J]. Optik, 2021, 242: 167186.

[3] Zhu X X, Wang W H, Jiang R S, et al. Research on ultrasonic-assisted drilling in micro-hole machining of the DD6 superalloy[J]. Advances in Manufacturing, 2020, 8(3): 405-417.

[4] Liu F, Li L, Zhang B, et al. A novel electrochemical sensor based on microporous polymeric nanospheres for measuring peroxynitrite anion released by living cells and studying the synergistic effect of antioxidants[J]. The Analyst, 2019, 144(23): 6905-6913.

[5] Sharmila G, Muthukumaran C, Kirthika S, et al. Fabrication and characterization of Spinacia oleracea extract incorporated alginate/carboxymethyl cellulose microporous scaffold for bone tissue engineering[J]. International Journal of Biological Macromolecules, 2020, 156: 430-437.

[6] Zeng X, Hu X, Song H, et al. Microwave synthesis of zeolites and their related applications[J]. Microporous and Mesoporous Materials, 2021, 323: 111262.

[7] Firsa T, Tadjuddin M, Udink A, et al. Effect of Machining Parameters on Hole Accuracy and Burr Formation in Micro-Drilling of Brass[J]. Defect and Diffusion Forum, 2020, 402: 73-80.

[8] Zhang Y, Qiao H, Zhao J, et al. Research on water jet-guided laser micro-hole machining of 6061 aluminum alloy[J]. The International Journal of Advanced Manufacturing Technology, 2022, 118(1-2): 1-13.

[9] Cung K, Bitsis D C, Briggs T, et al. Effect of Micro-Hole Nozzle on Diesel Spray and Combustion[C]//WCX World Congress Experience. 2018: 2018-01-0301.

[10] Huan L, Jicheng B, Yan C, et al. Micro-electrode wear and compensation to ensure the

dimensional consistency accuracy of micro-hole array in micro-EDM drilling[J]. The International Journal of Advanced Manufacturing Technology, 2020, 111(9-10): 2653-2665.

[11] Liu Y Z. Coaxial waterjet-assisted laser drilling of film cooling holes in turbine blades[J]. International Journal of Machine Tools and Manufacture, 2020, 150: 103510.

[12] Li Z, Bai J, Cao Y, et al. Fabrication of microelectrode with large aspect ratio and precision machining of micro-hole array by micro-EDM[J]. Journal of Materials Processing Technology, 2019, 268: 70-79.